Morphine Addiction and Its Withdrawal Effects on Prefrontal Cortex Using Concurrent Study of LFP and OISi

Leila Mohammadzadeh
Laser and Plasma research institute, Shahid Beheshti University
Amir Alizadeh
Neuroscience Research Center, School of Medicine
Mohammad Feiz
Laser and Plasma research institute, Shahid Beheshti University
Shole Jamali
Neuroscience Research Center, School of Medicine
Mohaddeseh Abedi
Department of Physics, Shahid Beheshti University
Abbas Haghparast
Neuroscience Research Center, School of Medicine
Hamid Latifi (latifi@sbu.ac.ir)
Laser and Plasma Research Institute, Shahid Beheshti University, Tehran, 1983969411, Iran

Research Article

Keywords: resting state functional connectivity (rsFC), local field potential (LFP), Opiates, cortices imaged

Posted Date: December 9th, 2020

DOI: https://doi.org/10.21203/rs.3.rs-118916/v1

Abstract

Opiates are among the widely abused substances worldwide. Also, the clinical use of opioids can cause unwanted and potentially serious consequences such as developing tolerance and dependence. In this study, we simultaneously measured the changes induced after morphine dependence and naloxone-induced withdrawal syndrome on the resting state functional connectivity (rsFC) and local field potential (LFP) power in prefrontal cortex of the rat. Our results revealed that acute morphine administration significantly increased the LFP power in all frequency bands as well as the rsFC strength of the prefrontal cortex, and naloxone injection reversed this effect. In contrast, chronic morphine administration reduced neural activity and general correlation values in intrinsic signals as well as the LFP power in all frequency bands. In addicted rats, after each morphine administration, the LFP power in all frequency bands as well as the rsFC strength of the prefrontal cortex were increased and these effects were further enhanced after naloxone precipitated withdrawal syndrome. We conclude that general correlation merely reflects the field activity of the local cortices imaged.

Introduction

Heroin and opium are two of the most widely abused opiates both for their euphoric and antinociceptive properties. Drug addiction is a serious health concern around the world and can cause psychological and financial damages [1,2]. Opium consumption in certain parts of Iran is part of local traditions and culture. Iran alone consumes 40% of the global opium. Moreover, despite the invention of new and safer painkillers such as NSAIDs, morphine is still an important clinical tool for managing severe and chronic pains, which is often associated with unwanted subsequences such as developing tolerance and dependence in patients. Morphine dependence causes many physiological changes in the brain and central nervous system. Therefore, understanding neurophysiology of addiction has been central to extensive research in Iran.

Up to now, brain imaging studies have played an important role in understanding the addictive properties of drugs. Some of these properties result from biological processes, particularly those in the brain's structure and function. However, the study of how different drugs affect certain brain areas and what areas of the brain are affected by these drugs needs further investigation[2]. The clinical and neuroimaging studies have found the effects of abuse drugs on temporal insula and thalamus[3], nucleus accumbens [4], amygdala [5], prefrontal [6], and sensorimotor [7] cortices. Another study has also revealed differences in the resting-state functional connectivity (rsFC) of the ganglia/limbic network in the resting-state before and after addiction to nicotine[8]. These abnormalities in rsFCs within this network may be related to improper rewarding effects in drug abusers.

Some studies [9–17] have found changes in functional and structural properties of the brain. However, the effects of long-term opioid drug usage have not been extensively studied. Many of these studies have used either functional imaging or electrophysiology techniques. Combining these two broad methods of acquiring brain activity can produce very interesting information and give us unprecedented insights into

how functional imaging relates to neuronal activity in general and how neoplastic changes during addiction may be better described using a combined approach, in particular.

The main goal of this work is to compare the effects of chronic and acute morphine consumption on the rsFC of the prefrontal cortex (PFC) using simultaneous optical imaging and LFP recording.

Functional connectivity (FC) expresses a statistical dependence between the brain signals [18]. In other words, two brain regions are functionally connected if they have synchronized or coherent dynamics [18–20]. The explanation of various measurements in the brain signals depends on the recordings method [2]. The FC measurements utilizing hemodynamic signals may help to system-level FC assessments. Indeed it can represent the neural interaction between different regions of the brain [21,22]. Whereas measurement of the FC by measuring the neuronal spikes may help to cell-level assessments. In other words, it could be expressed as functional connections between neurons [23]. The rsFC changes can potentially be useful in the assessment of different neuropsychiatric trajectories in drug abusers. The primary aim of studies related to brain activities in drug abusers is to investigate the neurophysiological variations among them[2]. The current work focuses on assessing the rsFC and neuronal activity measured by two recording methods: OISi and LFP. OISi is an optical imaging method to indirectly measure the brain activity by evaluating changes of the reflected light from the cortex and measuring the changes of the cerebral blood oxygenation [24,25]. Whereas the LFP recording is an effective electrophysiological method to check the neuronal activities [26]. Despite the effect of rsFC measurements in the diagnosis of different mental disorders, the rsFC has been assessed in a few addiction-related studies [2,27]. Using a combination of the OISi and the LFP recording in morphine-dependent rats, the convergence between the FC changes and the variations of the power of neuronal activities can be investigated. The rsFC based on OISi data can analyze the low-frequency oscillations of the intrinsic hemodynamic signals [22]. Furthermore, the resting state's brain networks are related to brain functions such as reward, cognitive or sensory processes [28]. Thus, by assessing the resting state brain networks, one can get fundamental information about the intrinsic function of the brain that may be helpful in recognizing the networks related to behaviors caused by addiction, which may be useful in therapeutic or diagnostic mechanisms.

The aim of the present study is to determine how the rsFC and the LFP strength of the PFC is affected by chronic and acute morphine abuse. We also intend to investigate the changes in these two factors resulting from chronic and acute morphine withdrawal using naloxone. If morphine abuse produces detectable changes in the rsFC of the PFC, then optical functional imaging methods with high spatial resolution may become an important biomedical methodology in drug abuse and clinical research. One of these imaging methods is OISi. This method can provide information about hemodynamic fluctuations of the brain. In this work, we combined the OISi and the LFP recordings from the PFC of the rat and tried to compare plastic changes undertaken after morphine addiction.

Results

Effects of acute morphine injection, morphine dependence, and naloxone-induced withdrawal syndrome on the rsFC of the PFC

On the experiment day, animals in both groups received a single dose of morphine followed by the naloxone injection. Simultaneously recordings of the OISi and LFP data were performed before and after each injection. Figure 1 shows the correlation and PCA maps of the morphine-addicted rats. Panels d, e, and f of Fig. 1 show the mean correlation values for baseline, after morphine injection, and after Naloxone-induced morphine withdrawal syndrome, respectively. Very significant improvement in correlation values after morphine injection, and even further increases in these values after naloxone injection are appeared compared to those of the baseline (pre-morphine) in PCA correlation maps (Panels g, h, and i of Fig. 1) as well as in general correlation maps (Panels a, b, and c of Fig. 1) and may indicate an overall increase in cortical FC. The results obtained using all three methods utilized to compute whole cortex's correlation map showed that the Naloxone injection significantly amplified effect of morphine injection in addicted rats (Figs. 1 and 3).

Acute morphine injection in the saline control group significantly increased the basic level of activity and, therefore, remarkably enhanced the rsFC strength in the PFC (Fig. 2). However, in contrast to the addicted rats, the naloxone injection failed to further enhance general, mean and PCA correlation values and significantly reversed the effect of morphine injection on the rsFC strength. (Details are provided in Supplementary Tables S1-S3). Notably, Naloxone injection significantly reversed effect of morphine injection in general correlation, mean correlation, and PCA values in this group (Figs. 2 and 3).

A comparison of intra- and inter-hemispheric rsFC values between addicted and saline control group is provided in Fig. 3. Panel (a) provides comparison of the general correlation values. Notably, there seems to be a stronger correlation within each hemisphere regardless of treatment compared with the rsFC strength between the two hemispheres. In addition, in the addicted group, while left and right hemispheres seem to be in a very close state of activity before morphine injection, the rsFC strength increases with morphine and naloxone injection, and the slope of the right hemisphere's rsFC is slightly sharper than that of the left hemisphere. However, in the saline group, morphine injection induces a greater activity in the right hemisphere (similar to the addicted rats). In this group, morphine enhanced intra- and inter-hemispheric rsFC values but naloxone injection reduces both intra- and inter-hemispherical brain activities.

As panels (b) and (c) of Fig. 3 demonstrate, mean and PCA values follow a similar pattern but with a stronger correlation overall.

The mean value and the standard deviation of rsFC strengths in the left and right hemisphere, across all regions included in the PFC, as well as the connectivity strength between two hemispheres were calculated using three mentioned correlation maps. These values were compared between different experimental conditions in both groups utilizing one-way ANOVA. The numerical and statistical results were reported in detail in the Supplementary Tables S1, S2, and S3. Furthermore, the rsFC strengths in pre-morphine and post-morphine conditions were separately compared between morphine dependent and

saline control rats (Supplementary Table S6). The results showed significant differences between the morphine and the saline group of rats in both conditions. The P-value and therefore the significance level of the statistical comparisons were shown in mentioned Supplementary Tables utilizing the symbols *, **, ***, ****, #, and n.s. for $P < 0.05$, $P < 0.01$, $P < 0.001$, $P < 0.0001$, $P < 0.00001$, and $P \geq 0.05$, respectively.

Effects of acute morphine injection, morphine dependence, and naloxone-induced withdrawal syndrome on the neural activity in the PFC.

Power spectra Plots of the LFP signal are plotted for the frequency intervals including Δ [0.1-4 Hz], θ [4–8 Hz], α [8–12 Hz], β [12–30 Hz], Low Y [30–80 Hz], and High Y [80–145 Hz]. Figure 4 sums up the average power of each band for pre-morphine, post-morphine, and post-naloxone injection conditions for morphine addicted and saline control groups. The mean value and the standard deviation of the LFP powers in all mentioned frequency bands were also calculated and compared between different experimental conditions utilizing One-Way ANOVA. The numerical values and the statistical results of One-Way ANOVA comparisons for both groups were reported in Supplementary Tables S4 and S5. In the saline control group, the acute morphine administration increased LFP power of all frequency bands and subsequent naloxone injection significantly reduced it (the P-values of the Bonferroni test between pre-morphine, post-morphine, and post-naloxone injections for Δ, θ, α, β, Low Y, and High Y frequency bands were symbolized in Supplementary Table S4). In contrast, in the morphine dependent group, the morphine injection increased average powerof LFP in all frequency bands (albeit not significantly), but naloxone-induced withdrawal syndrome manifested itself in the form of a very significant enhancement of LFP power in all frequency bands. The LFP powers in all frequency bands for pre-morphine and post-morphine conditions were also separately compared between morphine addicted and saline control rats (Supplementary Table S7). The results revealed remarkable differences between the morphine and saline group of rats in both conditions for all specified frequency ranges except for Y frequency bands.

The shape of the power spectra Plots of the LFP signals in all frequency bands were evaluated more carefully. These evaluations revealed remarkable changes in spectral shape of these signals for morphine dependent rats after naloxone injections (Supplementary Fig. S1). However, these investigations showed no significant changes in spectral shape of LFP signals in saline group of rats (Supplementary Fig. S2). It can be inferred from the results that the LFP signals showed the increased oscillatory behavior following naloxone injection in addicted rats.

Discussion

In the current work, the effects of morphine addiction on cortical network dynamics were compared using simultaneous intrinsic functional imaging and local field potential recordings. The results showed that: 1) acute administration of morphine significantly enhanced inter- and intra-hemispheric rsFC strength and this effect was reversed after naloxone administration. Same effect was also observed in LFP power average in all frequency bands. 2) Comparison of baseline rsFC (pre-morphine) values between addicted and saline control group suggests that long-term morphine administration reduced the overall rsFC

strength in the PFC. This effect was also present in the LFP activity of all frequency bands but on a significant degree. And 3) naloxone injection significantly reversed effects of morphine injection on both rsFC and LFP power values in saline group. However, the naloxone-induced morphine withdrawal syndrome in addicted rats, caused further increase in rsFC strength and LFP powers of all frequency bands. We showed for the first time that chronic morphine administration reduces baseline neural activity of prefrontal region of the rat which is manifested both in rsFC strength and LFP power values.

A previous study on the Nucleus Accumbens [29] (a key loci in mesolimbic system) showed similar increase in LFP powers after morphine injection. This observation can be (at least partially) explained by a situation in which overall network activity of the mesolimbic system is enhanced after an acute morphine injection. For instance, glutamatergic projections from the prefrontal cortex to the NAc [30] may (partially) explain these seemingly coordinated changes in the network. Such acute effect can be reversed by means of an opioid antagonist (naloxone) effectively reverses such situation. However, addiction to opiate seems to have very different effects on the brain which is not far from expectation [31]. In our data, this is indicated by the shift in baseline activity of the prefrontal cortex in addicted rats. Surprisingly, blockade of opioid receptors very significantly increases LFP powers.

The PFC is a key area for encoding and retrieving memory, cognitive functions [32], and addiction-associated behaviors [33] that received dopaminergic innervation from the ventral tegmental area [34]. Studies showed that VTA-dopaminergic signals on PFC through D1-like dopamine receptors enhance neuronal firing in PFC. Opioids, by acting on μ-opioid receptors, inhibit inhibitory interneurons and thereby increase the firing of the VTA-DA projections by disinhibition mechanism [35]. Therefore, there is a transient increase in DA release in the areas that innervate by VTA-DA projections, such as Accumbens and PFC [36]. Neural activity enhancement in PFC may be explained by the increased phasic dopamine release following the acute administration of morphine. Chronic morphine did not change the extracellular level of dopamine and noradrenaline in PFC [37]. Ning Liu. et al. demonstrated that EEG power in all frequency bands in PFC declined following chronic morphine-injection in monkeys [38]. In line with their results [38], in the present study, we also showed that LFP-power in all frequency-bands was decreased after morphine dependence in rats. Previous studies showed that the naloxone-injection increased the extracellular level of dopamine and noradrenaline within PFC in morphine-dependence rats while the concentration of these neuromodulators did not change following naloxone injection in the saline group [37]. Therefore, the increased oscillatory activity in PFC following naloxone injection in rats that received chronic morphine may be resulting from the elevated dopamine level in PFC after naloxone injection.

Overall, similarities between the pattern of changes in LFP power and rsFC strength indicate that the functional imaging signal in our study reflects general networks activity.

Methods

Experimental setup

Optical intrinsic signal imaging (OISi) and local field potential (LFP) recordings were obtained simultaneously in anesthetized rats. To this, the experimental OISi setup described in our last work [39] was used. In addition, an electrode connected to the LFP recording box was used to record the cortical electrical activity during imaging of the rat cortex.

Experimental procedures

Animals, Surgical Procedures And Data Recordings

Eighteen adult male Wistar rats (250–350 g) were housed under controlled temperature (22 ± 2 °C) and constant humidity with a 12-hour light/dark cycle. All animals had free access to chow and tap water and were caged individually. All testing procedures and treatments were conducted in accordance with the National Institute of Health and Guide for the Care and Use of Laboratory Animals (NIH Publications, revised in 2011) and were approved by the ethics in research committee of Shahid Beheshti Medical University. The current study was carried out in compliance with the ARRIVE guidelines (Animal Research: Reporting of In Vivo Experiments). The rats were randomly divided into three groups, each including six rats (behavioral control, saline, and morphine). The purpose of the behavioral control group preparation was solely to prove effectiveness of the morphine dependence protocol (data are not shown). All LFP and OISi experiments as well as all stages of data analysis were performed blindly to the details of animal grouping. The rats were first anesthetized with urethane (1.25 g/kg) to prepare for imaging. After removing the scalp, a 4 by 8 mm area of the skull on top of the PFC was thinned using a dental drill so much so the coronary arteries were fully visible. Afterward, using dental acrylics, a wall was created around the thinned cranial region of the cortex and was filled with artificial cerebrospinal fluid (ACSF) or saline to keep the surface arteries and the cortex clearly visible during the experiments. Then the precise position of the camera above the rat's brain was located by using an XYZ stage [24,25,39]. To record the LFPs, an electrode was fabricated by twisting a pair of stainless steel microwires (100 µM, 11 mm length) and inserted in the cortex via a small hole (0.5 mm diameter) drilled in the caudal quarter of the thinned area. LFP signals were amplified (1000x), bandpass filtered (0-300 Hz), and digitized (1 kS/s) using a commercially available data acquisition system and software (Niktek.ir). The animals' body temperature was kept at 37 °C using a thermal blanket throughout the experiment. Following the completion of the experiments, all animals were decapitated using a lab guillotine under deep anesthesia.

Development Of Morphine Dependence In Rats

Dependency to morphine was induced using the following protocol: Animals in the behavioral control and the morphine groups were received daily injections of morphine (25 µL, s.c, 2 times a day at 9:00 and 21:00) for 5 days. The protocol was started by 5 mg/kg injection for the first day (each daily injection contained 2.5 mg of morphine), and the injection dose was gradually increased during the consecutive days (10, 20, 30, and 40 mg/kg, from day 2 to day 5, respectively). The saline group was received daily doses of saline injetion (25 µL) under the exactly same schedule for 5 days. All animals were received a

single dose of morphine (40 mg/kg) on the testing day, 1 hour before surgery or 2 hours before the behavioral test in the case of the behavioral control group.

Morphine withdrawal syndrome was induced by a single injection of Naloxone (5 mg/kg, i.p), 2 hours after last morphine injection.

Morphine sulfate (Temad, Iran), Naloxone (Sigma, Germany), and Urethan (Sigma, Germany) were all prepared freshly to use on the same day.

Imaging protocol

The imaging protocol was explained in detail in our previous study [39]. After preparing the rats, imaging was performed at 80 fps. The imaging trials in the current study were done by imaging the cortex for about 20 minutes in resting-state conditions before- and after- morphine as well as after naloxone injection in both groups.

In this study, the prefrontal cingulate cortex (Bregma, -2.5 to 5.5 mm; Lateral, -2.0 to 2.0 mm) of the two groups (saline and morphine) of rats were imaged according to the Paxinos atlas of the rat brain [40]. The image of the PFC in which the LFP recording was also done, is shown in Fig. 5.

Analyzes

LFP signals analysis

The Chronux [41] toolbox for MATLAB (Mathworks, US) was used to analyze the LFPs. The spectral analysis was performed using the multi-taper method. Five Slepian tapers and a time-bandwidth product of 3 were used to achieve optimal spectral concentration. For each animal, the spectral power was computed before and after morphine and naloxone injection.

Intrinsic signals analysis: Calculating the functional connectivity based on the intrinsic signals

To calculate rsFC, each imaging trial was divided into four trials containing 300 s resting state experiments. The data of these experiments were analyzed to calculate the fractional value (FV) [39] of the reflected light from the cortex to assess the rsFC of the cortex.

As previously reported in our previous study [39], at first, as a pre-processing analysis before measuring the FC, a conventional regression method in the fMRI, known as “tCompCorr” global linear model analysis [42], was used to better interpret the correlating and non-correlating regions in the FC maps. Afterward, to obtain the rsFC of the cortex, the Pearson correlation between the FVs of the cortex regions was measured. To reduce the calculation volume, the images were segmented into blocks of 10 × 10 pixels and a time-related signal was assigned to each block by averaging its pixels’ FVs. Then, a bandpass filter in the frequency range of 0.009–0.08 Hz was applied to the signals [21,43–45]. The resulting signals were then used to measure the Pearson correlation between the blocks to evaluate the FC [43,46]. Finally, the

Fisher z-transformation was applied to the correlation coefficients [43] and then these coefficients were normalized between 0 and 1 in accordance with Peri's study [18] to obtain the limited and normalized coefficients.

Using the explained procedure, a large number (equal to the number of blocks) of the rsFC maps for each experimental condition (before- and after- morphine as well as after naloxone injection) was obtained. Each of these rsFC maps shows the functional connections between a block and the rest of the blocks included in the PFC image. In the present study, three methods were used to calculate the overall rsFC in the PFC. In the first method, each of the obtained rsFC maps was resized from the MxN matrix to a 1xMxN vector. These vectors were then placed in a larger matrix to create the "general correlation map". The resulting matrix has (MxN)x(MxN) components in which the elements of the first row show the correlation values between the first block and the rest of the blocks in the cortex image. Similarly, other elements of this matrix show the correlation values between every block of the cortex image with the rest blocks (Figs. 1 and 2 (a-c)). In the second method, the obtained FC maps were averaged on component by component and the "mean correlation map" was constructed (Figs. 1 and 2 (d-f)). As the third method, to obtain an overall rsFC map "principal component analysis" (PCA) method was applied. In this method, at first, every FC map was converted to a column vector. Afterward, the mean of these obtained vectors was computed on component by component basis, and then it was subtracted from any vectors. Next, the obtained vectors were placed in a bigger matrix. Afterward, the covariance matrix of the obtained big matrix was computed. Finally, the eigenvectors and eigenvalues of the covariance matrix were calculated. The eigenvalues were reordered in descending arrangement and in correspond to them, the eigenvectors were also reordered. By adding the mean vector to the eigenvectors, and then by converting the resulted vectors to the MxN matrices, the principal correlation matrices were computed. In the current study, by evaluating the ratio of the sum of the first three eigenvalues to the sum of all eigenvalues, it was inferred that the first three PCA matrices can be used to visualize 92% of the total functional connections between the PFC regions. In addition, by using the same evolutions for the first 15 eigenvalues, it was found that the first 15 PCAs could visualize 98% of the overall rsFC. In the current work, the first three PCAs were utilized to visualize the overall rsFC maps of the cortex as done in Mikula et.al. study [47]. The red, green, and blue colors were used to display PCA correlation maps. Utilizing this procedure, one can assign the RGB color combination to the set of blocks to produce a two-dimensional rsFC color map that can visualize the overall rsFC matrix of the PFC with relatively high accuracy. The red, green, and blue colors were assigned to the first, second, and third PCA correlation maps, respectively. In other words, in the obtained color map, the blocks with similar color denote the blocks with similar rsFC profiles. The obtained PCA correlation maps are shown in Figs. 1 and 2 (g-i).

Statistical analysis

After calculating the rsFC based on hemodynamic intrinsic signals and assessing the neuronal activity based on LFP power in the PFC, the rsFC and neuronal activity values were compared between different experimental conditions (before- and after- morphine as well as after naloxone injection) in the saline and

the morphine group of rats. The significance of the differences between the different experimental conditions in the two groups was measured using the one-way ANOVA. The normality and variance homogeneity of the data of each group were respectively examined by using the Kolmogorov–Smirnov and the Levene test as the required assumptions for parameter analysis. Bonferroni comparison tests were used for the post-hoc analyses. Differences with P□0.05 were considered statistically significant.

In order to statistically evaluate the changes induced in the rsFC of the PFC after -morphine and -naloxone injection in the experimental groups, the three methods mentioned in the previous section were used. So, one method to compare rsFC of the PFC between considered experimental conditions in the two groups is to compare the general correlation maps. Utilizing the general correlation matrix, the average value of the rsFCs across whole PFC, within each hemisphere, and between the two hemispheres were compared between the mentioned experimental conditions. The average rsFC across the whole of the PFC was measured by averaging the rsFC strength across all blocks included in the PFC image. The average rsFC within each hemisphere was also calculated by averaging the rsFC strengths across the blocks within each of the two hemispheres. Furthermore, the average of the rsFC strength between two hemispheres was also computed by measuring rsFC strength between each block in one hemisphere and each block in another hemisphere, and then by averaging them across all blocks included in one hemisphere. Another method to compare the rsFC of the PFC between considered experimental conditions is to compare the mean correlation maps. For statistical comparison, the mean values of the rsFC strengths within left and right hemisphere and across all blocks within the PFC were compared between all these experimental conditions in the two groups. These comparisons were done by averaging all rsFC strengths included in the left and right half as well as in whole of the mean correlation matrix, respectively. Finally, to numerically compare the rsFC values between considered experimental conditions, the average of the correlation strengths included in 15 first PCAs was utilized. In these comparisons, the average values of the rsFC within each hemisphere and across whole of the PFC were compared between mentioned experimental conditions in both groups.

In order to statistically assess variations induced in the neuronal activity of the PFC after -morphine and -naloxone injection, the average of the LFP power across Δ [0.1-4], θ [4–8], α [8–12], β [12–30], Low Y [30–80], and High Y [80–145] [48] frequency bands were compared between different experimental conditions in the two groups.

Declarations

Acknowledgments

This article has been extracted from Leila Mohammadzadeh PhD thesis and the preparation of experimental OISi setup to do this work was supported by the Cognitive Sciences and Technologies Council of Iran [grant number 101052-5].

Author Contributions

H.L. was responsible for the supervision, project leading, funding acquisition, visualization, validation, and interpretation of findings. L.M. was responsible for the investigation, methodology, resources, software, preparation the rats for experiments, data acquisition, data analysis, original draft preparation, interpretation of findings, and writing the manuscript. A.H. contributed to the study design and conceptualization, and interpretation of findings. A.M.A. contributed the experimental setup preparation, data acquisition, software, revising the manuscript, and interpretation of findings. M.S.F. contributed to the experimental setup preparation. Sh.J. contributed to the data acquisition and interpretation of findings. M.A. contributed to the rats' preparation for experiments and data acquisition. All authors critically reviewed content and approved final version for publication.

Competing Interests: The authors declare no competing interests.

DATA AVAILABILITY

The data that support the findings of this study are available from the corresponding author on request.

References

1. Bart, G. Maintenance medication for opiate addiction: the foundation of recovery. *Journal of addictive diseases* **31**, 207–225 (2012).
2. Ieong, H. F.-h. & Yuan, Z. Resting-state neuroimaging and neuropsychological findings in opioid use disorder during abstinence: a review. *Frontiers in human neuroscience* **11**, 169 (2017).
3. Goldstein, R. Z. & Volkow, N. D. Drug addiction and its underlying neurobiological basis: neuroimaging evidence for the involvement of the frontal cortex. *American Journal of Psychiatry* **159**, 1642–1652 (2002).
4. Noel, M. B. & Gratton, A. Electrochemical evidence of increased dopamine transmission in prefkontal cortex and nucleus accumbens elicited by ventral tegmental μ-opioid receptor activation in freely behaving rats. *Synapse* **21**, 110–122 (1995).
5. Baxter, M. G., Parker, A., Lindner, C. C., Izquierdo, A. D. & Murray, E. A. Control of response selection by reinforcer value requires interaction of amygdala and orbital prefrontal cortex. *Journal of Neuroscience* **20**, 4311–4319 (2000).
6. Parvaz, M. A., Alia-Klein, N., Woicik, P. A., Volkow, N. D. & Goldstein, R. Z. Neuroimaging for drug addiction and related behaviors. *Reviews in the Neurosciences* **22**, 609–624 (2011).
7. Liu, J. *et al.* Dysfunctional connectivity patterns in chronic heroin users: an fMRI study. *Neuroscience letters* **460**, 72–77 (2009).
8. Janes, A. C., Nickerson, L. D., Frederick, B. d. & Kaufman, M. J. Prefrontal and limbic resting state brain network functional connectivity differs between nicotine-dependent smokers and non-smoking controls. *Drug and alcohol dependence* **125**, 252–259 (2012).

9. Ryan, A., Molloy, F., Farrell, M. & Hutchinson, M. Fatal toxic leukoencephalopathy: clinical, radiological, and necropsy findings in two patients. *Journal of Neurology, Neurosurgery & Psychiatry* **76**, 1014–1016 (2005).
10. Offiah, C. & Hall, E. Heroin-induced leukoencephalopathy: characterization using MRI, diffusion-weighted imaging, and MR spectroscopy. *Clinical radiology* **63**, 146–152 (2008).
11. Ma, N. *et al.* Addiction related alteration in resting-state brain connectivity. *Neuroimage* **49**, 738–744 (2010).
12. Robinson, T. E. & Kolb, B. Morphine alters the structure of neurons in the nucleus accumbens and neocortex of rats. *Synapse* **33**, 160–162 (1999).
13. Luo, F. *et al.* Attenuation of brain response to heroin correlates with the reinstatement of heroin-seeking in rats by fMRI. *Neuroimage* **22**, 1328–1335 (2004).
14. Xi, Z. X., Wu, G., Stein, E. A. & Li, S. J. Opiate tolerance by heroin self-administration: An fMRI study in rat. *Magnetic Resonance in Medicine: An Official Journal of the International Society for Magnetic Resonance in Medicine* **52**, 108–114 (2004).
15. Liao, D., Lin, H., Law, P. Y. & Loh, H. H. Mu-opioid receptors modulate the stability of dendritic spines. *Proceedings of the National Academy of Sciences* **102**, 1725–1730 (2005).
16. Cunha-Oliveira, T. *et al.* Street heroin induces mitochondrial dysfunction and apoptosis in rat cortical neurons. *Journal of neurochemistry* **101**, 543–554 (2007).
17. Shabat-Simon, M., Levy, D., Amir, A., Rehavi, M. & Zangen, A. Dissociation between rewarding and psychomotor effects of opiates: differential roles for glutamate receptors within anterior and posterior portions of the ventral tegmental area. *Journal of Neuroscience* **28**, 8406–8416 (2008).
18. Peri, E. *Functional Connectivity Based Framework for Analysis and Visualization of FMRI Data*. (Tel Aviv University, 2008).
19. Whitfield-Gabrieli, S. & Nieto-Castanon, A. Conn: a functional connectivity toolbox for correlated and anticorrelated brain networks. *Brain connectivity* **2**, 125–141 (2012).
20. Paasonen, J., Stenroos, P., Salo, R. A., Kiviniemi, V. & Gröhn, O. Functional connectivity under six anesthesia protocols and the awake condition in rat brain. *Neuroimage* **172**, 9–20 (2018).
21. Yoshida, Y., Nakao, M. & Katayama, N. Resting-state functional connectivity analysis of the mouse brain using intrinsic optical signal imaging of cerebral blood volume dynamics. *Physiological measurement* **39**, 054003 (2018).
22. Bauer, A. Q. *et al.* in *Biomedical Optics*. BM4A. 7 (Optical Society of America).
23. Ray, S. & Maunsell, J. H. Network rhythms influence the relationship between spike-triggered local field potential and functional connectivity. *Journal of Neuroscience* **31**, 12674–12682 (2011).
24. Chen-Bee, C. H., Agoncillo, T., Xiong, Y. & Frostig, R. D. The triphasic intrinsic signal: implications for functional imaging. *Journal of Neuroscience* **27**, 4572–4586 (2007).
25. Pouratian, N. Optical imaging based on intrinsic signals. *Brain mapping*, 97–140 (2002).

26. Gabriel, M., Julien, C., Salin, P. A. & Jean-Christophe, C. Differential recordings of local field potential: A genuine tool to quantify functional connectivity. *PloS one* **13** (2018).
27. Sutherland, M. T., McHugh, M. J., Pariyadath, V. & Stein, E. A. Resting state functional connectivity in addiction: lessons learned and a road ahead. *Neuroimage* **62**, 2281–2295 (2012).
28. Schmidt, A. *et al.* Increased functional connectivity in the resting-state basal ganglia network after acute heroin substitution. *Translational psychiatry* **5**, e533-e533 (2015).
29. Soleimani, S. M. A. *et al.* Acute morphine administration alters the power of local field potentials in mesolimbic pathway of freely moving rats: Involvement of dopamine receptors. *Neuroscience letters* **686**, 168–174 (2018).
30. Pierce, R. C. & Kumaresan, V. The mesolimbic dopamine system: the final common pathway for the reinforcing effect of drugs of abuse? *Neuroscience & biobehavioral reviews* **30**, 215–238 (2006).
31. Dejean, C., Boraud, T. & Le Moine, C. Opiate dependence induces network state shifts in the limbic system. *Neurobiology of disease* **59**, 220–229 (2013).
32. Peters, G. J., David, C. N., Marcus, M. D. & Smith, D. M. The medial prefrontal cortex is critical for memory retrieval and resolving interference. *Learning & memory* **20**, 201–209 (2013).
33. Brenhouse, H. C., Lukkes, J. L. & Andersen, S. L. Early life adversity alters the developmental profiles of addiction-related prefrontal cortex circuitry. *Brain sciences* **3**, 143–158 (2013).
34. Cooper, S., Robison, A. & Mazei-Robison, M. S. Reward circuitry in addiction. *Neurotherapeutics* **14**, 687–697 (2017).
35. Johnson, S. & North, R. Opioids excite dopamine neurons by hyperpolarization of local interneurons. *Journal of neuroscience* **12**, 483–488 (1992).
36. Patriarchi, T. *et al.* Ultrafast neuronal imaging of dopamine dynamics with designed genetically encoded sensors. *Science* **360** (2018).
37. Devoto, P., Flore, G., Pira, L., Diana, M. & Gessa, G. Co-release of noradrenaline and dopamine in the prefrontal cortex after acute morphine and during morphine withdrawal. *Psychopharmacology* **160**, 220–224 (2002).
38. Liu, N. *et al.* EEG activities in the orbitofrontal cortex and dorsolateral prefrontal cortex during the development of morphine dependence, tolerance and withdrawal in rhesus monkeys. *Brain research* **1053**, 137–145 (2005).
39. Mohammadzadeh, L. *et al.* Measuring the Frequency-Specific Functional Connectivity Using Wavelet Coherence Analysis in Stroke Rats Based on Intrinsic Signals. *Scientific Reports* **10**, 1–18 (2020).
40. Paxinos, G., Watson, C. R. & Emson, P. C. AChE-stained horizontal sections of the rat brain in stereotaxic coordinates. *Journal of neuroscience methods* **3**, 129–149 (1980).
41. Bokil, H., Andrews, P., Kulkarni, J. E., Mehta, S. & Mitra, P. P. Chronux: a platform for analyzing neural signals. *Journal of neuroscience methods* **192**, 146–151 (2010).
42. Behzadi, Y., Restom, K., Liau, J. & Liu, T. T. A component based noise correction method (CompCor) for BOLD and perfusion based fMRI. *Neuroimage* **37**, 90–101 (2007).

43. Vincent, J. L. *et al.* Intrinsic functional architecture in the anaesthetized monkey brain. *Nature* **447**, 83 (2007).
44. White, B. R. *et al.* Resting-state functional connectivity in the human brain revealed with diffuse optical tomography. *Neuroimage* **47**, 148–156 (2009).
45. Bauer, A. Q. *et al.* Optical imaging of disrupted functional connectivity following ischemic stroke in mice. *Neuroimage* **99**, 388–401 (2014).
46. Lee Rodgers, J. & Nicewander, W. A. Thirteen ways to look at the correlation coefficient. *The American Statistician* **42**, 59–66 (1988).
47. Mikula, S. & Niebur, E. A novel method for visualizing functional connectivity using principal component analysis. *International journal of neuroscience* **116**, 419–429 (2006).
48. Jia, X. & Kohn, A. Gamma rhythms in the brain. *PLoS Biol* **9**, e1001045 (2011).

Figures

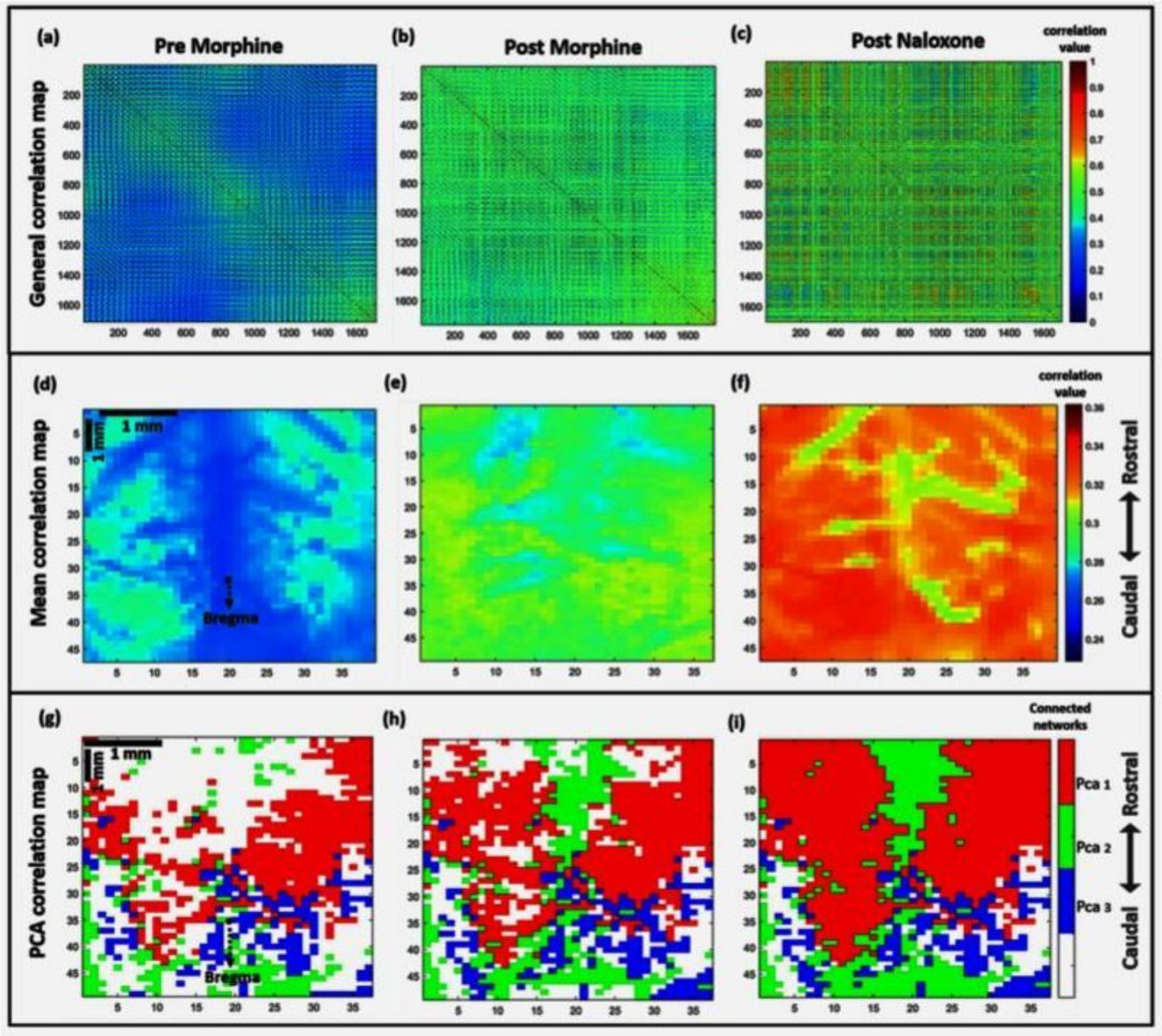

Figure 1

The "General correlation map" for (a). pre morphine, (b). post morphine, and (c). post naloxone conditions, the “Mean correlation map” for (d). pre morphine, (e). post morphine, and (f). post naloxone conditions, and the “PCA correlation map” for (g). pre morphine, (h). post morphine, and (i). post naloxone conditions in morphine dependent rats. The first, second, and third principal correlation networks were shown in red, green, and blue, respectively. The coordinate of the Bregma and the spatial scale bars on cortex images were shown in panels (d) and (g).

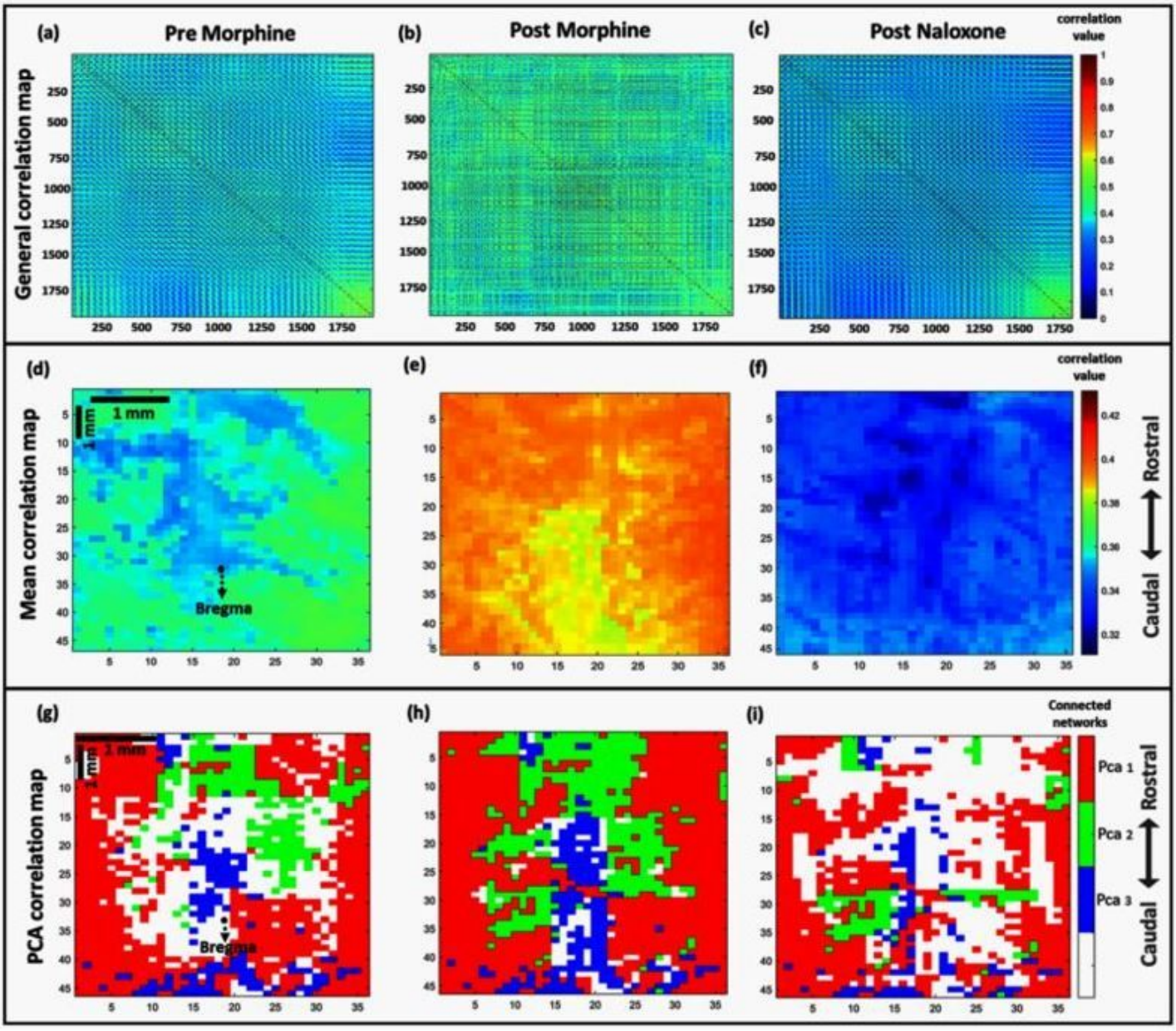

Figure 2

The "General correlation maps" for (a). pre morphine, (b). post morphine, and (c). post naloxone conditions, the “Mean correlation maps” for (d). pre morphine, (e). post morphine, and (f). post naloxone conditions, and the “PCA correlation maps” for (g). pre morphine, (h). post morphine, and (i). post naloxone conditions in the saline group of rats. The first, second, and third principal correlation networks were shown in red, green, and blue, respectively. The coordinate of the Bregma and the spatial scale bars on cortex images were shown in panels (d) and (g).

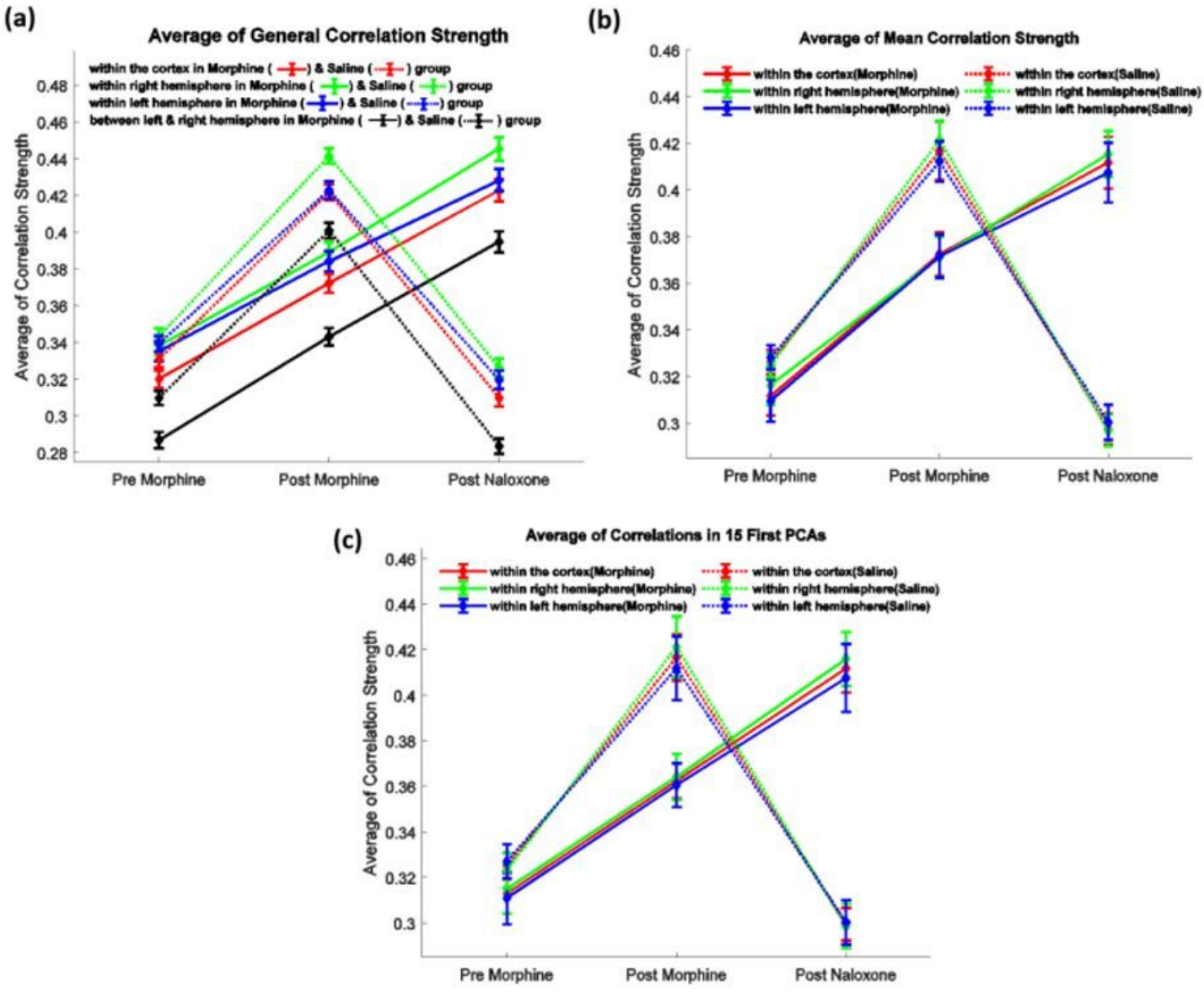

Figure 3

The changes of the FC strength utilizing (a). “General Correlation” , (b). “Mean Correlation” , and (c). “average of first15 PCA” maps after morphine and naloxone injection in saline (dash line) and morphine (solid line) group of rats: The mean and the standard deviation of the FC values at all experimental conditions are illustrated in this figure. STD indicate the error bars or variations between pixels’ FC strengths. The FC strength within the right and the left hemisphere are shown in green and blue, respectively. The FC strength within the whole of the prefrontal cortex are shown in red. The FC strength between the left and the right hemispheres are shown in black. The numerical values were reported in Supplementary Table S2.

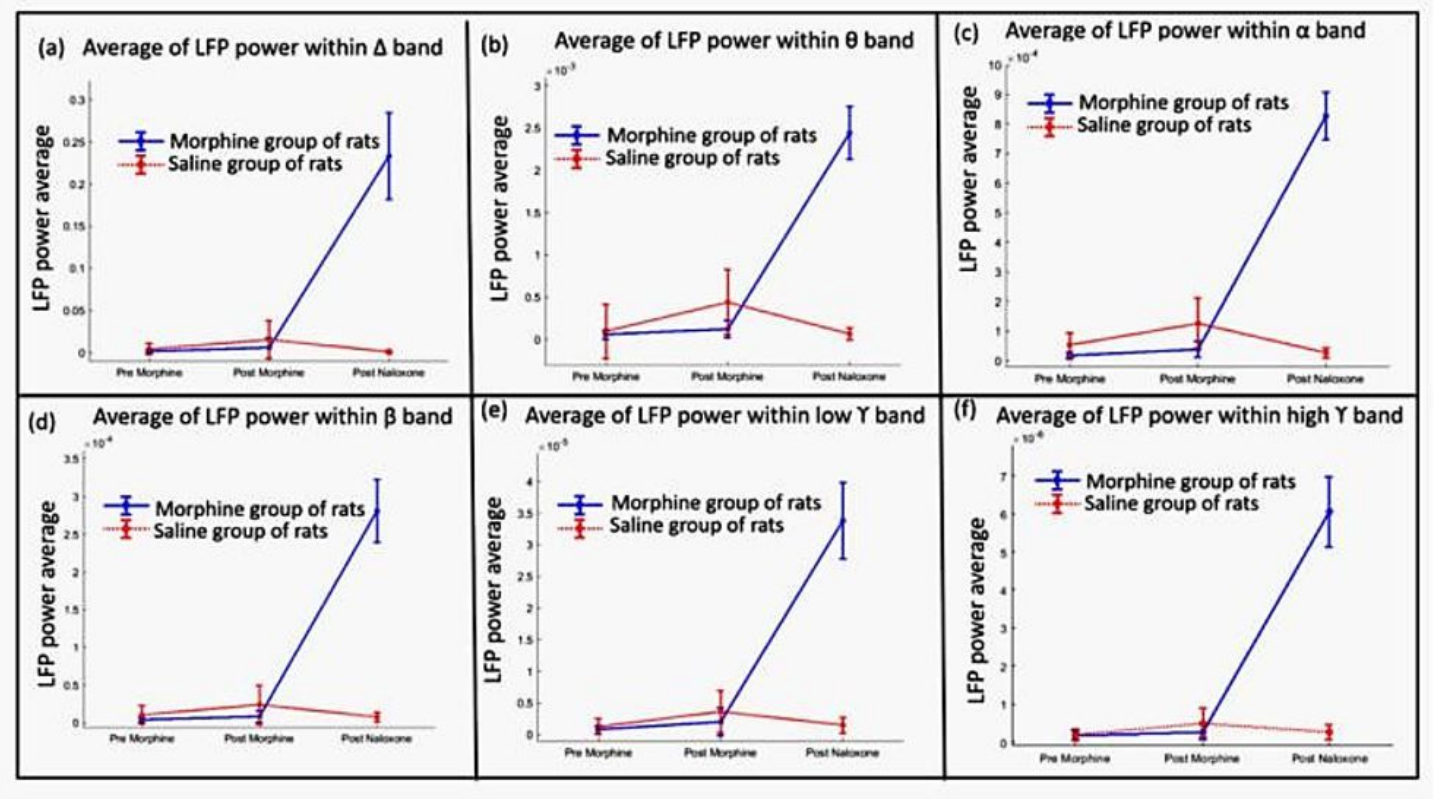

Figure 4

Changes of the LFP power average in both group for six frequency domains before and after morphine and naloxone injections: The mean and the standard deviation of the LFP powers at all experimental conditions are illustrated in this figure. P-values and the numerical values of the LFP power average were reported in supplementary Tables S4 and S5, respectively.

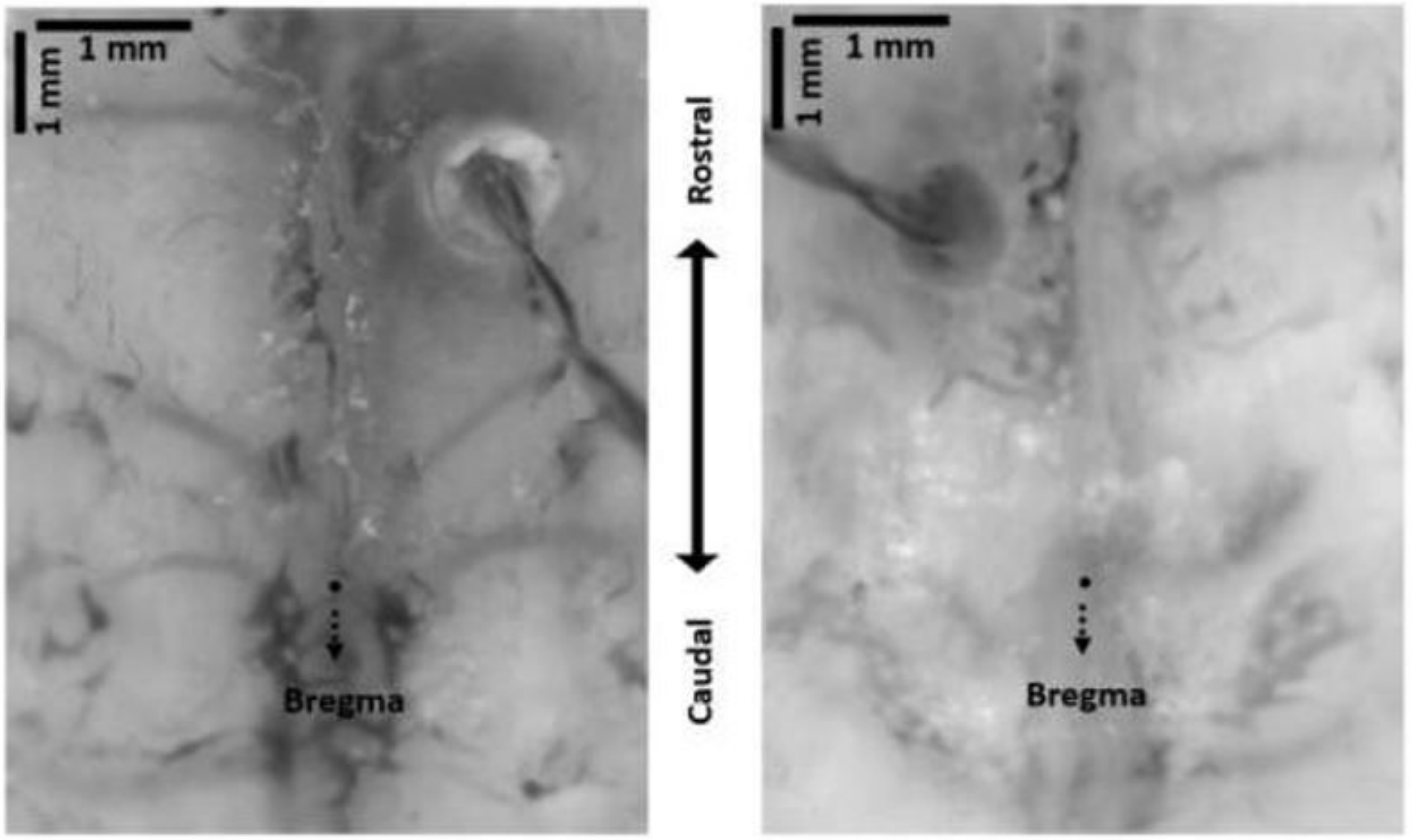

Figure 5

The image of Prefrontal cortex (PFC). For each group of rats, for half of the total number of experiments, the LFP electrode were inserted in the right hemisphere and for the remaining half, in the left hemisphere of the brain and recorded the electrical activity of the PFC. The coordinate of the Bregma, the rostral-caudal direction, and the spatial scale bars are shown in this figure.

Supplementary Files

This is a list of supplementary files associated with this preprint. Click to download.

- Supplementryfilecompressed.docx